

EFFECTS OF MOIST FROUDE NUMBER AND OROGRAPHIC ASPECT RATIO ON A CONDITIONALLY UNSTABLE FLOW OVER A MESOSCALE MOUNTAIN

Shu-Hua Chen¹, Yuh-Lang Lin², Zhan Zhao¹ and Heather Dawn Reeves²

¹Department of LAWR, University of California, Davis, CA 95616-8627

²Department of MEAS, North Carolina State University, Raleigh, NC 27695

Email: *shachen@ucdavis.edu*

Abstract: A series of idealized simulations for an unsaturated, conditionally unstable flow over a two-dimensional mountain ridge were performed to investigate how the unsaturated moist Froude number (F_w) and the aspect ratio of mountain height to half-width (h/a), affect the propagation, cloud type and rainfall amount of orographically induced precipitation systems. The moist Froude number (F_w) was varied by increasing or decreasing the basic state wind speed (U) while the aspect ratio was varied by increasing or decreasing the mountain half-width (a). For low F_w flows, the flow is in an upstream propagating regime and shows little or no sensitivity to changes in a . For moderate or large values of F_w , the flow shifts more toward a downstream propagating regime as a is decreased (i. e. as h/a is increased). The domain integrated accumulated precipitation was not sensitive to the aspect ratio. For a fixed h/a , the flow shifts more toward a downstream propagating flow regime as F_w is increased, a result that is consistent with previous research. Additionally, the results show that there is an increase in the domain integrated precipitation as F_w is increased.

Keywords - ICAM, MAP, Croatia

1. INTRODUCTION

In order to improve quantitative precipitation forecasts for orographic rain associated with conditionally unstable flow over a mesoscale mountain, it is important to understand the basic dynamics associated with it. It has been found that several flow and orographic parameters, such as F_w ($F_w = U/N_w h$; Chu and Lin 2000), CAPE, aspect ratio, moisture content, and vertical distribution of moisture, dictate the nature of orographically induced convective systems. For example, Chu and Lin (2000) identified three moist flow regimes for two-dimensional flow over a mesoscale mountain. Chen and Lin (2005a) extended that work to three-dimensional flow over an idealized Alpine mountain and found that a strong low-level flow is able to produce large accumulations of precipitation over the upslope of the 3-D mountains, which is consistent with observations and the findings of Chu and Lin (2000). Finally, Chen and Lin (2005b) investigated the combined effects of F_w and CAPE and identified four flow regimes: (1) Regime I: flow with an upstream propagating convective system and an early, slowly moving convective system over the mountain; (2) Regime II: flow with a long-lasting orographic convective system over the mountain peak, upslope or lee slope; (3) Regime III: flow with an orographic convective or mixed convective and stratiform precipitation system over the mountain and a downstream propagating convective system; and (4) Regime IV: flow with an orographic stratiform precipitation system over the mountain and possibly a downstream propagating cloud system. Note that the fourth regime (IV) was not included in the flow regimes proposed by Chu and Lin (2000) and Chen and Lin (2005a). In this study, we will consider the effects of the mountain aspect ratio (h/a) and F_w on the formation and propagation of precipitation systems associated with conditionally unstable flow over a two-dimensional, mesoscale mountain.

2. MODEL DESCRIPTION AND EXPERIMENTAL DESIGN

The Weather Research and Forecasting (WRF) model version 2.0 (Chen and Dudhia 2000; Skamarock et al.

2001), which is a compressible, 3D, nonhydrostatic model, was used for all simulations presented herein. The governing equations for the WRF model are written in flux-form, and mass and dry entropy are conserved. Terrain-following mass coordinates ($\sigma - p$) are used. The Runge-Kutta third-order time scheme and fifth and third order advection schemes are chosen in the horizontal and vertical directions, respectively. An open (radiative) lateral boundary condition in the north-south direction, a free-slip lower boundary condition, and a periodic boundary condition in the east-west are chosen. In the horizontal direction, the domain is extended 1000 km with a grid spacing of 1 km while in the vertical direction, the grids are stretched with a total of 51 points from 1000 hPa on the surface to model top (about 20 km). The Purdue-Lin microphysics parameterization scheme and turbulence kinetic energy diffusion scheme are activated in all simulations. A 5-km deep sponge layer is added to the upper part of the physical domain to reduce artificial wave reflection. The idealized, two-dimensional mountain geometry is given by

$$h_{sfc} = \frac{ha^2}{[(x - x_o)^2 + a^2]} \quad (1)$$

where h_{sfc} is the terrain height, h is the mountain peak height (2 km) and a is the mountain half-width. The mountain is introduced impulsively into the basic flow at the time the simulation is started. All simulations were integrated for 10 h with a time step of 1 s.

The initial conditions are horizontally homogeneous. The sounding used in Chen and Lin (2005b), which has a CAPE about 3000 J kg⁻¹, is used. The unsaturated moist Brunt-Väisälä frequency (N_w), given by

$$N_w^2 = \frac{g}{\bar{\theta}_v} \frac{\partial \theta_v}{\partial z} \quad (2)$$

where θ_v is the virtual potential temperature, is approximately 0.0095 s⁻¹. Note, N_w was estimated from the surface to approximately 3 km in a column far upstream from the mountain ridge and $\bar{\theta}_v$ is the mean virtual potential temperature of this layer.

In order to study the effects of F_w and h/a on the formation and propagation of orographically induced convective systems, a two-dimensional matrix of experiments was devised wherein first the basic state wind, U , was varied in order to vary F_w . For these experiments, a was held constant. The values of U that were used are 2.5, 5, 7.5, 10, 15, 20 and 30 m s⁻¹ which correspond to F_w s of 0.131, 0.262, 0.393, 0.524, 0.786, 1.048, and 1.572, respectively. In the second set of experiments, a was varied from 7.5, 15, 22.5, 30, and 45 km. In all experiments, h was 2 km. A summary of all experiments performed can be found in Table 1.

Table 1: The classification of flow regimes with respect to the unsaturated moist Froude number (F_w) and the aspect ratio. The mean basic wind and the half mountain width corresponding to each case are identified in the parentheses. (A1, A2, A3, A4, A5) correspond to the aspect ratio = (2/7.5, 2/15, 2/22.5, 2/30, 3/45), and (F1, F2, F3, F4, F5, F6, F7) correspond to $F_w = (0.131, 0.262, 0.393, 0.524, 0.786, 1.048, 1.572)$.

	A1 (7.5 km)	A2 (15 km)	A3 (22.5 km)	A4 (30 km)	A5 (45 km)
F1 (2.5 m s ⁻¹)	I	I	I	I	I
F2 (5 m s ⁻¹)	I	I	I	I	I
F3 (7.5 m s ⁻¹)	I	I	I	I	I
F4 (10 m s ⁻¹)	II	I	I	I	I
F5 (15 m s ⁻¹)	III	III	II	II	II
F6 (20 m s ⁻¹)	III	III	III	III	III
F7 (30 m s ⁻¹)	IV	IV	III	III	III

3. RESULTS AND DISCUSSION

Let us first consider the flow response when a is held constant while U is varied. When h/a is fixed, the flow

transitions to a higher numbered regime as F_w is increased. This result is consistent with previous studies (Chu and Lin 2000; Chen and Lin 2005b). It is also found that a slightly larger F_w is required for the regime transition to occur when the aspect ratio (mountain width) becomes smaller (larger) (i. e., column A1 vs. column A5 in Table 1). This can be understood through comparison of the advective time scale ($\tau_{adv} = 4a/U$) with the cloud time scale ($\tau_{cloud} \cong 1200$ s). As a is increased (i. e. h/a is decreased), τ_{adv} increases which implies convective systems have a longer residence time on the upstream side of the mountain. In consequence, a stronger cold pool can be produced to act against the basic-state flow. This further acts to propel the flow to a low numbered regime. Therefore, a larger F_w is required in order to shift the flow toward a higher numbered regime.

One unique result uncovered from the simulations with varying F_w is that of the domain integrated accumulated rainfall. When the basic wind speed is large compared to the mountain half-width, τ_{adv} is very small and the flow becomes non-hydrostatic. In the extreme case of $a = 7.5$ km and $U = 30$ m s⁻¹, $\tau_{adv} \sim 1000$ s which is shorter than τ_{cloud} . Hence, there was insufficient time for convective cloud development in airstreams as they crossed the orography and the overall precipitation was less than in neighboring cases in the flow regime diagram (Table 1; A1F6 and A2F7).

Now let us consider what happens when F_w is held constant while a is varied. According to Table 1, the flow regime classification is not dependent on the aspect ratio if F_w is small (i. e. $U \leq 7.5$ m s⁻¹). This is because the basic flow is hydrostatic and the basic state wind is too weak to overcome the barrier presented by the mountain. Although all cases with $U \leq 7.5$ m s⁻¹ are classified as belonging to regime I, the accumulated precipitation patterns can be quite different as is shown in Fig. 1. This figure shows the 10 h accumulated precipitation for cases A1F3 to A5F3. For each simulation, the main or primary precipitation maximum is located over or near the mountain peak. Each simulation also has a secondary maximum located between 100 and 200 km upstream of the mountain peak. The larger the mountain half-width, the farther upstream this secondary maximum is positioned. The explanation for this is relatively straight-forward. When the mountain half-width is increased, the area of lifting is much broader and the leading convective cell is located farther upstream. This, along with a stronger cold pool as mentioned earlier (i.e., longer advection time), explains why the convective system can propagate further upstream when the half mountain width is increased.

Although the spatial distributions of the total rainfall amounts are very different for the different cases presented in Fig. 1, this does not have strong impact on the domain integrated rainfall amount. In other words, the domain integrated rainfall amount is almost independent of the half mountain width during the 10h simulation if the basic mean wind speed is fixed. This can be observed in Fig. 2, which shows domain integrated accumulated rainfall at even hours for A1F3 to A5F3. Notice that at each time shown, the accumulated precipitation amounts are very similar in each simulation. In fact, this conclusion is applicable to every case examined here except for A1F7 ($U = 30$ ms⁻¹ and $a = 7.5$ km) whose accumulated rainfall is smaller than A2F7 to A5F7 during the entire 10h simulation (figure not shown). The reason is due to small advection time when flow crosses the mountain for this case.

When F_w is increased above 0.393 ($U \geq 7.5$ m s⁻¹), the precipitation pattern and nature of convection are dictated by both F_w and h/a . According to Table 1, as a is increased, the flow shifts toward a lower flow regime. This dependence on h/a appears to be linked to nonhydrostatic effects. As discussed above, the wider the half-width, the longer τ_{adv} which implies the convective system has more time to develop over the upstream side of the mountain leading to stronger upstream cooling that can act to shift the flow to a

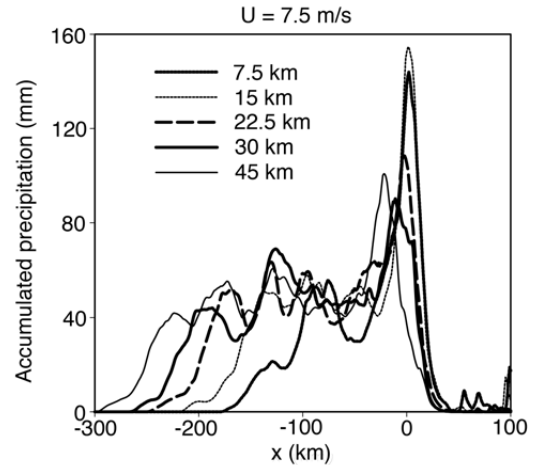


Figure 1: Spatial distribution of total accumulated rainfall (mm) after 10-h simulations for the mountain half width of 7.5 km (thick dashed line), 15 km (thin dashed line), 22.5 km (thick long-dashed line), 30 km (thick solid line), and 45 km (thin solid line). The basic wind speed is 7.5 ms⁻¹ and the mountain height is 2 km.

lower numbered regime.

4. CONCLUDING REMARKS

Idealized simulations for an unsaturated, conditionally unstable flow over a two-dimensional mountain ridge were performed to investigate how the unsaturated moist Froude number (F_w) and the orographic aspect ratio, which is defined as the ratio of mountain height to half-width (h/a), affect the propagation, cloud type and rainfall amount of orographically induced precipitation systems. This was tested through a series of idealized simulations using the Weather Research and Forecast (WRF) model wherein the basic uniform wind (i.e. F_w) and the mountain half-width (a) were varied. The simulation results indicate that for low F_w , the flow is insensitive to h/a and the flow is in an upstream propagating flow regime. For large F_w , both F_w and h/a dictate the precipitation pattern and the nature of the convection, with flow shifting more toward a downstream propagating regime with increasing h/a if F_w is fixed. This dependence on h/a for larger wind speeds appears to be linked to nonhydrostatic effects. With a fixed h/a , the flow shifts more toward a downstream propagating regime with increasing F_w .

It is also found that the domain integrated rainfall is sensitive to basic wind speed, in particular for those weak basic winds when the mountain half-width is fixed. On the other hand, the domain integrated accumulated rainfall is not sensitive to the aspect ratio (or the mountain half-width) when the moist Froude number (i.e., basic wind speed) is fixed.

Acknowledgments: *The authors would like to acknowledge the WRF model development team for their efforts in developing this model. This research is supported by NSF Grant ATM-0344237.*

REFERENCES

- Chen, S.-H., and J. Dudhia, 2000: Annual report: WRF physics [Available at <http://wrf-model.org>]
- Chen, S.-H., and Y.-L. Lin, 2005a: Orographic effects on a conditionally unstable flow over an idealized three-dimensional mesoscale mountain. *Meteor. Atmos. Phys.*, **88**, 1-21.
- Chen, S.-H. and Y.-L. Lin, 2005b: Effects of the basic wind speed and CAPE on flow regimes associated with a conditionally unstable flow over a Mesoscale Mountain, *J. Atmos. Sci.*, **62**, 331-350.
- Chu, C.-M., and Y.-L. Lin, 2000: Effects of orography on the generation and propagation of mesoscale convective systems in a two-dimensional conditionally unstable flow. *J. Atmos. Sci.*, **57**, 3817-3837.
- Skamarock, W. C., J. B. Klemp, and J. Dudhia, 2001: Prototypes for the WRF (Weather Research and Forecast) model. Ninth Conf. Meso. Processes, AMS, J11-J15 (also see <http://www.wrf-model.org>).

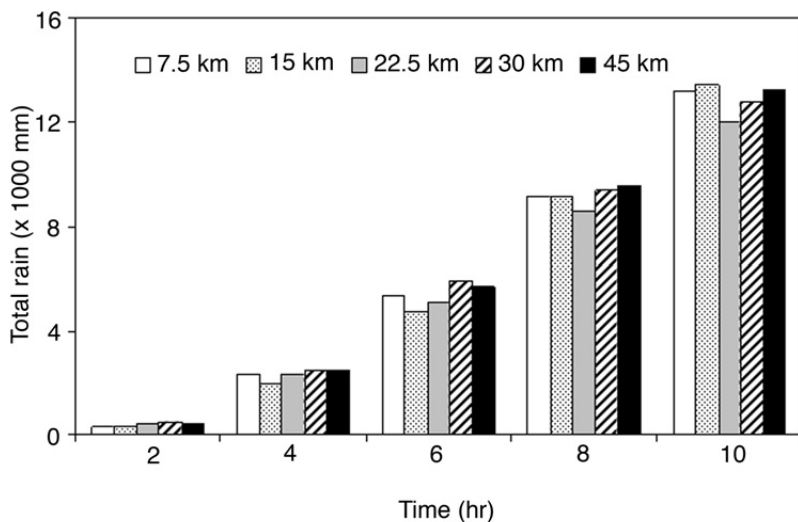


Figure 2: Accumulated total rainfall ($\times 1000$ mm) after 2h, 4h, 6h, 8h, and 10h integration for the half mountain width of 7.5 km (white), 15 km (hatched), 22.5 km (gray), 30 km (hatched), and 45 km (black-filled). The basic wind speed is 7.5 ms^{-1} and the mountain height is 2 km.